11. Cowin, S. C., "On the Strength Anisotropy of Bone and Wood," *J. Applied Mechanics, ASME Transactions*, Vol. 46, No. 4, pp. 832–837 (1979).

12. van der Put, T. A. C. M., "A General Failure Criterion for Wood," IUFRO Timber Engineering Group Meeting, Paper 23 [Sweden, 1982], IUFRO, Vienna.

13. U.S. Department of Agriculture, Forest Service, Forest Products Laboratory. "Wood Handbook: Wood as an Engineering Material," Agric. Handb. 72, Gov't Printing Office, Washington, D.C. (1974).

14. Daniel, I. M., "Behavior of Graphite/Epoxy Plates with Holes Under Biaxial Loading," *Experimental Mechanics*, Vol. 20, No. 1, pp. 1–8 (1980).

15. Daniel, I. M., "Biaxial Testing of $[0_2/\pm45]_s$ Graphite/Epoxy Plates with Holes," *Experimental Mechanics*, Vol. 22, No. 5, pp. 188–195 (1982).

A Symmetric Rail Shear Test for Mode II Fracture Toughness (G_{IIC}) of Composite Materials—Finite Element Analysis

H. V. LAKSHMINARAYANA
Scientist, Structures Division
National Aeronautical Laboratory
Bangalore 560 017 India

(Received September 26, *1983)*
(Revised January 19, 1984)

ABSTRACT

Using a high precision triangular finite element model, the elastic stress field in a symmetric rail shear test specimen is determined. The results are graphically presented and discussed. A simple finite element technique for energy release rate analysis of the pre-cracked test specimen is presented. Numerical results showing the effects of material properties and crack length are tabulated as normalized stress-intensity factors. Based on this numerical study it is fair to say that the symmetric rail shear test with some modifications is a viable method for shear characterization of composite materials in general and for G_{IIC} determination in particular. Final acceptance of the test method, however, awaits experimental verification.

1. INTRODUCTION

A GREAT IMPROVEMENT IN DAMAGE TOLERANCE OF COMPOSITE LAMinates can be achieved by using improved matrix materials. The specific property which accounts for such an improvement is identified as the interlaminar fracture toughness. When measuring interlaminar fracture toughness of unidirectional composite materials, a distinction between the opening mode (G_{IC}) and inplane sliding mode (G_{IIC}) values must be noted. A double cantilever beam test [1,2] is a viable method for measuring G_{IC}. The objective of this study is to provide a critical assessment of a symmetric rail shear test [3,4] for measuring G_{IIC}.

Figure 1 shows a sketch of the test set up. The test specimen is a flat unidirectional laminate of uniform thickness h with steel rails bolted (or bonded) leaving two test sections between rails of width b and length l. The force P applied to the central rail is transferred to each test section as inplane

0021-9983/84/03 0227—12 $4.50/0

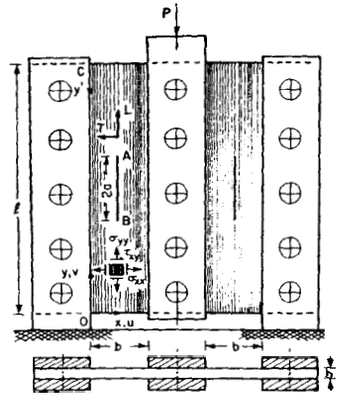

Figure 1. *Symmetric rail shear test specimen and fixtures.*

shear force. An aspect ratio l/b of ten, chosen for the present study was based on the analysis of Whitney et al [5]. A crack of length 2a is introduced at the center of each test section and the crackplane coincides with the fiber direction in the test specimen.

Finite element analysis can be used to make more informed decisions regarding the design of test specimen and fixtures before launching experimental investigations. Furthermore, a rigorous energy release rate analysis of the pre-cracked specimen is essential for reliable reduction of recorded test data. In particular, the effect of specimen geometry, crack length, material properties, and boundary conditions on the energy release rate denoted by G must be quantified. Finite element analysis happens to be an ideal tool for this purpose too.

TRIPLT is the acronym for a shear flexible triangular laminated composite plate finite element and the associated structural analysis program that was exclusively used in the present study. The research and rationale leading to the development of TRIPLT is well documented in Reference [6] and hence only the salient features are summarized here. The element illustrated in Figure 2 has three nodal points located at its vertices and 15 degrees of freedom are associated with each node. The mathematical formulation takes into account anisotropic elastic behaviour of constituent plies, bending–stretching coupling, and transverse shear deformation effects. Complete cubic polynomials are used to approximate the three displacement components (u,v,w) and two rotations (θ_x, θ_y) within the element. The displacements and rotations along with their first derivatives are chosen as the nodal parameters, enabling direct evaluation of stress resultants at the nodes. The versatility and computational efficiency of TRIPLT in providing accurate numerical solutions to some problems in mechanics of composites has been demonstrated [6,7]. In this study, TRIPLT was used to determine the

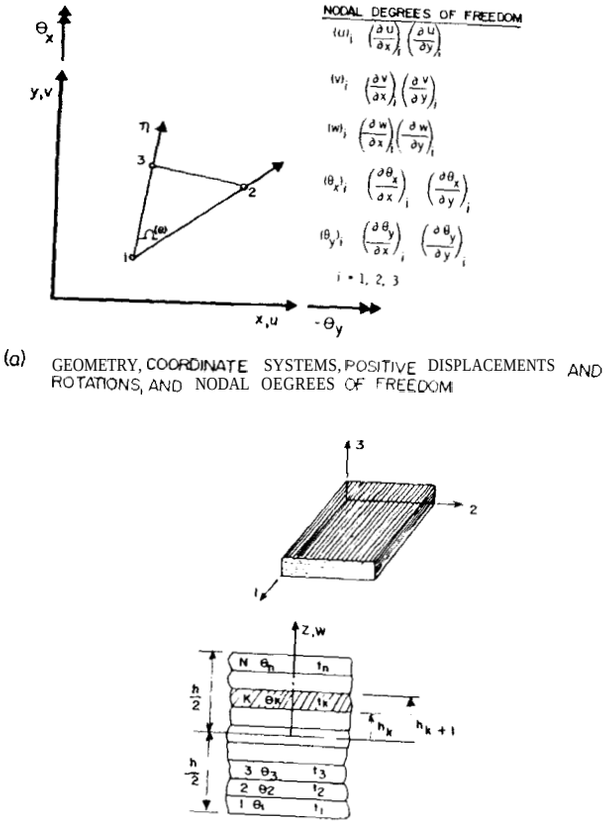

Figure 2. *Shear flexible triangular laminated composite plate finite element-TRIPLT.*

elastic stress field in the test specimen. Exploiting the pure membrane character of the stress field, all the bending degrees of freedom were suppressed in the analysis. The results obtained are graphically presented and discussed in the next section.

From an elastic energy balance consideration, Irwin [8] shows that the strain energy released during a small incremental crack extension is equal to the work done in closing the crack to its original length. This statement in equation form is the well-known crack closure integral. A finite element technique to calculate the energy release rate $G = G_I + G_{II}$, based on computing the crack closure integral, has been presented by Rybicki and

Kanninen [9]. The accuracy (for a given mesh) and computational effort (for acceptable accuracy) of this technique can be considerably improved by employing a high order finite element such as TRIPLT instead of constant strain elements as advocated by Rybicki and Kanninen. The significant advantages of the proposed method are: (1) it avoids dealing with the details of singular stress distribution around the crack tip where there are the added complexities of material anisotropy; (2) it permits separation of G into its components G_I and G_{II} in a mixed mode problem; (3) it assures high accuracy even with a coarse mesh; and (4) it permits the use of a general purpose finite element structural analysis program and does not require "singular elements." Further details of the technique, relevant to this study are presented in a subsequent section.

After evaluating G_I and G_{II}, well known relationships [10] are employed to calculate the associated stress intensity factors denoted by K_I and K_{II}. It is a matter of convenience to tabulate the numerical solutions as normalized stress intensity factors for various crack lengths and for different material systems. Such results are essentials for a consistent and reproducible reduction of test data.

Based on the results obtained in this study, it is fair to say that the symmetric rail shear test with some modifications is a viable method for shear characterization of composite materials in general and for the measurement of mode II fracture toughness (G_{IIC}) in particular. Final acceptance of the test method, however, awaits experimental verification.

2. STRESS ANALYSIS

Finite Element Model

The uncracked specimen was discretized using the 8 × 14 mesh of TRIPLT elements as shown in Figure 3(a). Clamped edge conditions were enforced at all nodes along $X = 0$ (i.e. $u = 0$, $\partial u/\partial y = 0$, $v = 0$, $\partial v/\partial y = 0$), while the nodes along the edge $X = b$ were constrained to move in the y direction. The nodes along the edges $y = 0$ and $y = 1$ were left unrestrained to simulate the traction-free conditions. The finite element model comprises of 135 grid points, 224 elements, and 720 degrees of freedom.

The accuracy of calculated stresses by the finite element method depends in addition to the number of elements used on their distribution. In particular a finemesh of small elements is necessary in regions where steep stress gradients and stress concentrations are expected. Apriori knowledge about the location of such regions in the test specimen prompted the choice of the mesh illustrated in Figure 3(a). Incidentally, Figure 3(b) illustrates a finite element model of the pre-cracked test specimen to be discussed subsequently.

Results and Discussion

Effective modulii of typical composite material systems used in the present study are given in Table 1. The stress distribution in a glass/epoxy composite

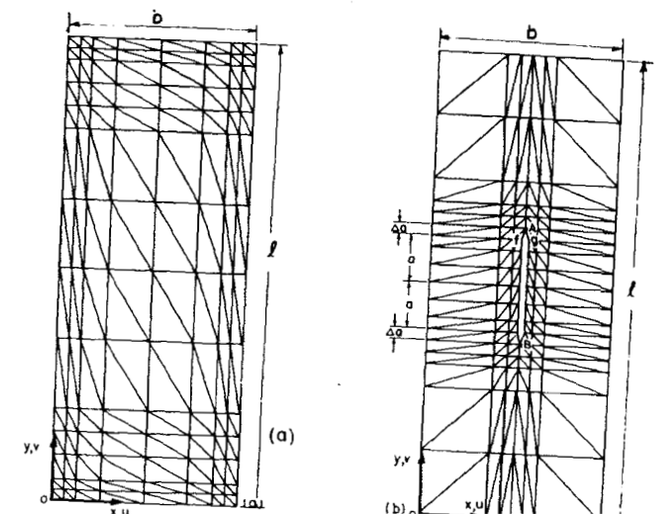

figure 3. TRIPLT finite element models of the test specimen: (a) for stress analysis; (b) for energy release rate analysis.

(scotchply 1002) specimen is presented in Figure 4, but some explanation is necessary to its understanding. The stress components σ_{xx}, σ_{yy} and τ_{xy} are normalized with respect to the nominal shear stress $\tau = P/2lh$, where P is the load applied by the testing machine to the central rail. The desired state of pure shear (i.e. $\sigma_{xx} = 0$, $\sigma_{yy} = 0$, $\tau = \tau$) is closely approximated in the test specimen except in a small region located near the free edges $y = 0$ and $y = 1$. In these regions, the stress field is highly complex. The shear stress increases from zero to its maximum value in a distance of about 1/10 as shown in Figure 4(b). Consequently, a significant amount of normal stress σ_{xx} is induced. Variation of the normal stress σ_{xx} at and near the edge $y = 1$, il-

Table 1. Unidirectional composite material properties used in the present study

Modulii	Glass/Epoxy (Scotchply 1002)	Graphite/Epoxy (AS-1/3502)	Graphite/Epoxy (T300/5208)	HM Graphite/Epoxy
E_L, 10^6 psi	5.8	21.0	26.25	30.0
E_T, 10^6 psi	1.2	1.65	1.5	0.75
G_{LT}, 10^6 psi	0.6	0.7	1.04	0.45
ν_{LT}	0.26	0.3	0.28	0.25

Conversion to SI units: 10^6 psi = 6.8948 GPa.

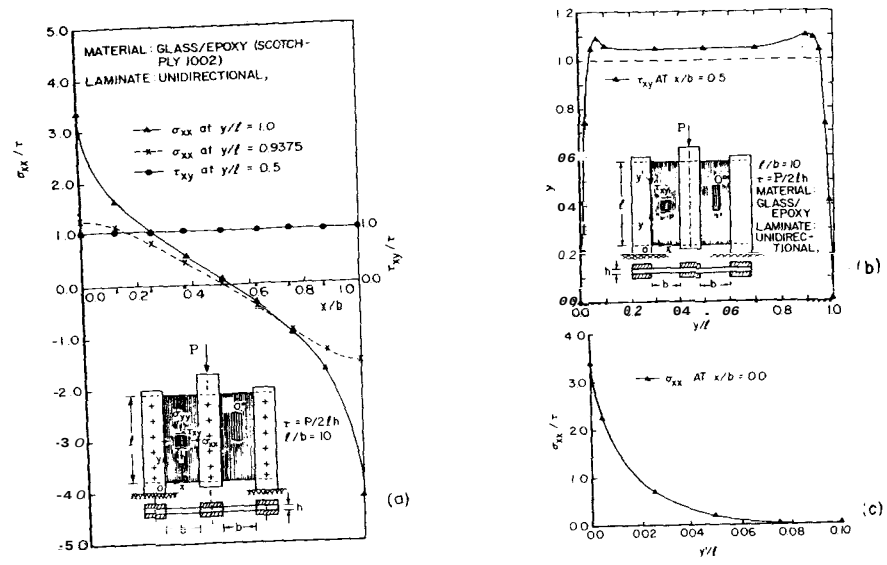

Figure 4. *Stress distribution in the glass/epoxy composite specimen.*

lustrated in Figure 4(a), clearly identifies regions of stress concentration close to the rails. The singular nature of the stress field in these regions is demonstrated in Figure 4(c), which shows the decay of σ_{xx} along the clamped edge. Notably, in the gage section of the specimen, the shear stress τ_{xy} is uniform and its magnitude is about 1.05 τ and the normal stresses σ_{xx} and σ_{yy} are very small.

The results presented in Figure 5 were obtained for a graphite/epoxy composite (As-1/3502) specimen. In general the stress field is similar to that of a glass/epoxy composite specimen. In the gage section, the uniform shear stress is seen to be equal to the nominal shear stress τ.

Failure analysis of the specimen was carried out using the simple maximum stress failure criterion. Since the transverse tensile strength of a unidirectional composite is lower than its inplane shear strength, it was evident that premature failure of the test specimen will initiate at the point C (Figure 1) in the transverse tension mode much before the onset of shear failure can take place in the gage section. This inability of the test to yield a failure mode for which it was intended precludes any meaningful interpretation of recorded test data. Obviously, modifications of the specimen and/or fixtures is essential to prevent this undesirable feature. A simple artifice of locally reinforcing the test specimen using some layers of woven cloth is believed to serve the purpose. The efficacy of the proposed modification is best verified by tests and hence no analysis was performed.

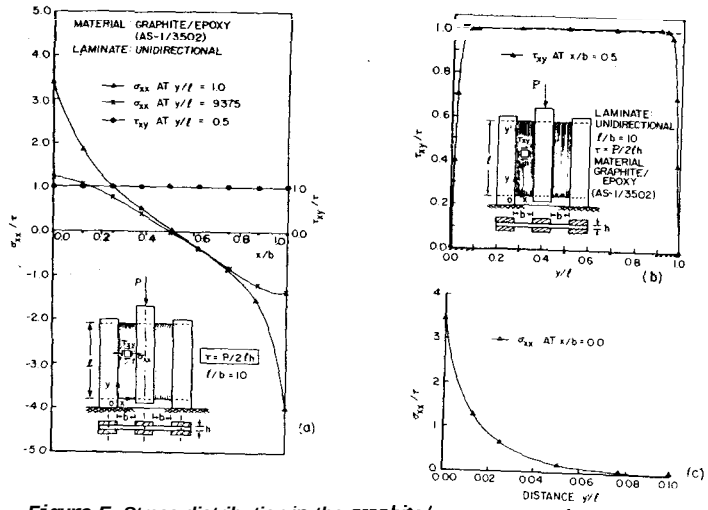

Figure 5. *Stress distribution in the graphite/epoxy composite specimen.*

The symmetric railshear test with the above modification appears to meet the requirements of an ideal test for shear characterization of composite materials. It is simple to conduct, requires small and easily fabricated specimens, the fixtures are reusable, and is suitable for the determination of shear stress-shear strain response to failure, shear modulus, and ultimate shear strength in a single test. This test can also be used to measure the mode II fracture toughness (G_{IIC}) of unidirectional composite materials by introducing a through crack at the center of the specimen and parallel to the direction of fibers (Figure 1). As the applied load P is gradually increased, it eventually reaches a point at which the specimen will fracture (failure due to crack propagation). The shear stress at this point is the fracture stress, τ_c and the corresponding value of the energy release rate, G_{IIC} is the mode II fracture toughness of the material. Determination of G_{IIC} from the test data, however, necessitates an energy release rate analysis of the pre-cracked specimen.

3. ENERGY RELEASE RATE ANALYSIS

Finite Element Model

The precracked test specimen was discretized using the **6** × 18 mesh of TRIPLT elements shown in Figure 3(b). Clamped edge conditions (i.e. $u = 0$, $\partial u/\partial y = 0$, $v = 0$, $\partial v/\partial y = 0$) were enforced at all the nodes along the edge $x = 0$, while the nodes along $X = b$ were constrained to move in the y direction. The nodes along $y = 0$ and $y = 1$ and along the crack surfaces were unconstrained to simulate the traction-free conditions. The finite element model thus comprises of 140 grid points, 216 elements, and 726 degrees of freedom.

The accuracy of the calculated energy release rate $G = G_I + G_{II}$ by the present method of analysis depends, in addition to the finite element mesh, on the value of the incremental crack extension, Δa, used in the computations. In particular, Δa must be sufficiently small in comparison with a, the half-crack length. A value of $\Delta a/a = 0.025$, used in the present study, was found to provide accurate solutions to a number of bench mark problems with known solutions. For example, Figure 6 compares the analytical solution of Kanninen [11] for a double cantilever beam test specimen (homogeneous isotropic material) with the numerical results from the present analysis. The two solutions are seen to be in good agreement over a range of crack lengths.

Evaluation of G_I and G_{II}

Figure 3(b) illustrates the finite element representation of the crack tip regions. Here, a small incremental crack extension Δa has been introduced by replacing the crack tip node (say A) with two separate nodes f and g. The first finite element solution yields the nodal displacements u_f, v_f, u_g, and v_g, under prescribed loading and boundary conditions. Equal and opposite nodal forces of magnitudes unity, parallel and perpendicular to the plane of the initial crack are then applied at the nodes f and g and the previous analysis is repeated. Combining the results of these two steps, the components of nodal forces F_x and F_y, the x and y-forces that are required to hold the nodes f and g together are determined. The work done to close the crack to its original length is approximated by

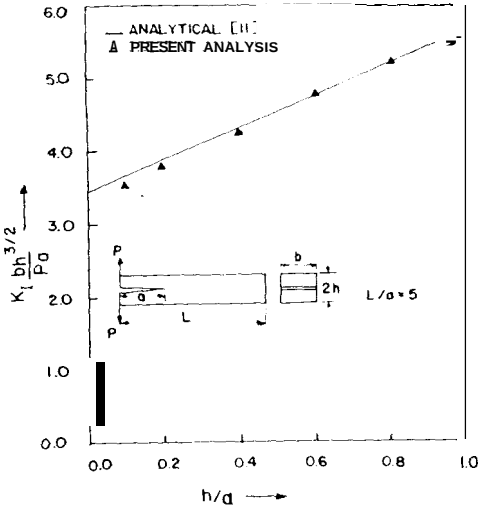

Figure 6. Comparison of numerical results with analytical solutions for a double cantilever beam test specimen.

$$\Delta W = [F_x (u_f - u_g) + F_y (v_f - v_g)]/2$$

Thus, the mode I (G_I) ad mode II (G_{II}) components of the energy release rate G are given by [9]:

$$G_I = \lim_{\Delta a \to o} \frac{1}{2h\Delta a} F_x (u_f - u_g)$$

and

$$G_{II} = \lim_{\Delta a \to o} \frac{1}{2h\Delta a} F_y (v_f - v_g)$$

A similar procedure holds good for the crack tip at B.

Results and Discussions

After evaluating G_I and G_{II}, the following relationships [10] are employed to calculate the corresponding crack tip stress intensity factors denoted by K_I and K_{II}.

$$G_I = \frac{K_I^2}{\sqrt{2E_L E_T}} \left[\left(\frac{E_L}{E_T}\right)^{1/2} + \frac{E_L}{2G_{LT}} - \nu_{LT} \right]^{1/2}$$

$$G_{II} = \frac{K_{II}^2}{E_L \sqrt{2}} \left[\left(\frac{E_L}{E_T}\right)^{1/2} + \frac{E_L}{2G_{LT}} - \nu_{LT} \right]^{1/2}$$

Where E_L and E_T denote the Young's modulii in the fiber and transverse directions respectively, G_{LT} is the in-plane shear modulus and ν_{LT} is the major Poisson's ratio.

It is a matter of convenience to tabulate the so calculated stress intensity factors as normalized values

$$y_I = \frac{K_I}{\tau\sqrt{a}}$$

and

$$y_{II} = \frac{K_{II}}{\tau\sqrt{a}}$$

It is informative to note that for an infinite plate with a small crack of length 2a at the center and loaded with in-plane shear stress τ at infinity, $Y_I = 0.0$

and $Y_{II} = \sqrt{\pi}$. Obviously, any deviation of the tabulated values of Y_I and Y_{II} from these will reflect the effects of specimen geometry (l/b), crack length (2a/1), material properties (E_L, E_T, G_{LT}, ν_{LT}), and boundary conditions on the stress intensity factors and hence on the energy release rate.

Numerical experiments were first performed to study the effect of material orthotropy on the energy release rate. The results presented in Table 2 were obtained for a specimen with $l/b = 10$ and $2a/1 = 0.2$. A closer look at these results lead to the following observations: (1) the stress intensity factors at the crack tips A and B (Figure 1) are not equal and the small difference is attributed to the unsymmetrical boundary conditions with respect to the crack plane; (2) The mode I component of the stress intensity-factor is not identically zero. However, the magnitude of K_I is very, very small in comparison with K_{II} so as not to have any significant influence on measured value of G_{IIC}; (3) the effect of composite material properties (effective modulii) on the stress intensity factors is insignificant; and (4) the computed values of Y_{II} for the composite material specimens do not deviate from the known infinite plate solution by more than three Percent.

Table 3 shows the effect of increasing crack length on the normalized stress intensity factors. These results were obtained for a graphite/epoxy (AS-1/3502) specimen with $l/b = 10$. The results are in conformity with the first two observations made in the previous paragraph. The manner in which the mode II stress intensity factor K_{II} varies as the crack length is increased is illustrated in Figure 6.

Based on the results obtained in the present study it is evident that in the symmetric rail shear test, the crack propagation will be mainly under mode I1 conditions as desired. However, care has to be taken to prevent the occurrence of premature failure in transverse tension close to the rails.

Table 2. Effect of material properties on the normalized stress intensity factors y_{II} and y_I. Symmetric rail shear test specimen with $l/b = 10$, $2a/l = 0.2$.

	Crack tip A		Crack tip B	
Material	$y_{II} = \frac{K_{II}}{\tau\sqrt{a}}$	$y_I = \frac{K_I}{\tau\sqrt{a}}$	$y_{II} = \frac{K_{II}}{\tau\sqrt{a}}$	$y_I = \frac{K_I}{\tau\sqrt{a}}$
Isotropic ($\nu = 0.3$)	1.9657	0.0936	1.9276	0.0399
Glass/Epoxy (scotchply 1002)	1.8255	0.0326	1.8084	0.0223
Graphite/Epoxy (T300/5208)	1.8063	0.0213	1.7969	0.0082
HM Graphite/Epoxy	1.7869	0.0111	1.7996	0.0041

Table 3. Effect of crack length on the normalized stress intensity factors y_{II} and y_I. Symmetric rail shear test specimen with $l/b = 10$. Material graphite/epoxy (AS-1/3502).

	Crack Tip A		Crack Tip B	
$\frac{2a}{l}$	$y_{II} = \frac{K_{II}}{\tau\sqrt{a}}$	$y_I = \frac{K_I}{\tau\sqrt{a}}$	$y_{II} = \frac{K_{II}}{\tau\sqrt{a}}$	$y_I = \frac{K_I}{\tau\sqrt{a}}$
0.2	1.8057	0.0190	1.7933	0.0091
0.3	1.8118	0.0113	1.8166	0.0079
0.4	1.8564	0.0128	1.8766	0.0191
0.5	1.9731	0.0107	1.9931	0.0213
0.6	2.1434	0.0219	2.1583	0.0067

4. SUMMARY AND CONCLUSIONS

The versatility and accuracy of TRIPLT in the determination of two-dimensional elastic stress field in a symmetric rail shear test specimen is demonstrated in this study. The complexity of the stress field at and near the free edges is evident from the numerical results that are graphically represented. However, in the gage section of the specimen, a state of pure shear is closely approximated.

A simple finite element technique for the calculation of energy release rate, based on **TRIPLT** finite element model and computation of crack closure integral was evaluated and used in the present study. Numerical results showing the effects of crack length and composite material properties on the energy release rate are tabulated as normalized stress intensity factors. Such results are essential for the determination of G_{IIC} from the test data.

Based on the present study, it is fair to conclude that a modified symmetric rail shear test is a viable method for shear characterization of composite

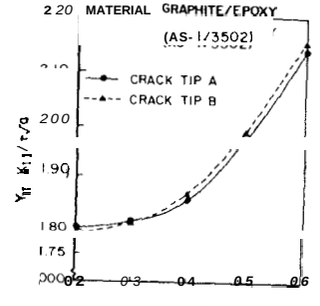

Figure 7. Variation of mode II stress intensity factor with crack length. Symmetric rail shear test specimen with $l/b = 10$.

materials in general and for G_{IIC} determination in particular. Final acceptance of the test method, however, awaits experimental investigations. The complementary role played by finite element analysis and experimental verification in the development of test methods for composite materials needs no emphasis.

ACKNOWLEDGEMENTS

The work reported in this paper was carried out during the author's tenure as NRC-AFSC Research Associate at Materials Laboratory, Air Force Wright Aeronautical Laboratories, Wright Patterson Air Force Base, Ohio 45433, USA. Sincere thanks are due to Dr. S. W. Tsai and Dr. J. M. Whitney for encouragement and useful discussions.

REFERENCES

1. Whitney, J. M., Browning. C. E., and Hoogsteden, W., "A Double Cantilever Beam Test for Characterizing Mode I Delamination of Composite Materials," *Journal of Reinforced Plastics and Composites,* pp. 297–313 (1982).
2. Wilkins, D. J., et al., "Characterizing Delamination Growth in Graphite-Epoxy," in *Damage in Composite Materials,* ASTM STP 775, pp. 168–183 (1982).
3. Tarnopolskii, Yu M., and Kincis, T., "Comparative Evaluation of Shear Test Methods for Composites," in *Fracture Mechanics of Composite Materials,* G. C. Sih and V. P. Tamuzs (editors), Martinus Nijhoff Publishers, The Hague, 1982.
4. Sims, D. F., "In-plane Shear Stress-Strain Response of Unidirectional Composite Materials," *Journal of Composite Materials,* Vol. 7, pp. 126–128 (January 1972).
5. Whitney, J. M., Standsbarger, D. L., and Hewell, H. B., "Analysis of the Rail Shear Test—Applications and Limitations," *J. Composite Materials,* Vol. 5, pp. 26–34 (January 1971).
6. Lakshminarayana, H. V., and Sridharamurthy, S., "A Shear-flexible Triangular Finite Element Model for Laminated Composite Plates," *International Journal for Numerical Methods in Engineering* (in press).
7. Lakshminarayana, H. V., "Stress Distribution Around a Semicircular Edge-Notch in a Finite Size Laminated composite Plate Under Uniaxial Tension," *Journal of Composite Materials,* Vol. 17, pp. 357–367 (July 1983).
8. Irwin, G. R., "Fracture," *Handbuck Der Physik*, Vol. 16, pp. 551 (1958).
9. Rybicki, E. F., and Kanninen. M. F., "A Finite Element Calculation of Stress Intensity Factors by a Modified Crack Closure Integral," *Engineering Fracture Mechanics,* Vol. 9, No. 4, pp. 931–938 (1977).
10. Sih, G. C., and Liebowitz, H., "Mathematical Theories of Brittle Fracture," in *Fracture, Vol. II, Mathematical Fundamentals,* H. Liebowitz (editor). Academic Press, New York, 1968.
11. Kanninen, M. F., "An Augmented Double Cantilever Beam Model for studying—Crack Propagation and Arrest," *International Journal of Fracture,* Vol. 9, pp. 83–92 (1973).

A Stochastic Model for the Growth of Matrix Cracks in Composite Laminates

A. S. D. WANG, P. C. CHOU AND S. C. LEI
Department of Mechanical Engineering and Mechanics
Drexel University
Philadelphia, PA 19104

(Received August 22. 1983)
(Revised February 15. 1984)

ABSTRACT

This paper presents a stochastic simulation model for the growth of multiple matrix cracks in composite laminates subjected to both static and fatigue loads. Working within the premise of ply-elasticity, a new concept of effective flaws is introduced which replaces the conventional constant ply strength criterion. Thus, the model consists of an application of fracture mechanics and a rational representation of material flaw distributions. Simulation examples are presented on $[0_2/90_2]_s$ and $[0_2/90_3]_s$ graphite-epoxy laminates which undergo characteristic transverse cracking under uniaxial tension.

INTRODUCTION

DAMAGE DEVELOPMENT IN FIBER REINFORCED COMPOSITE LAMINATES IS a very complicated process [1,2]. For polymer-based, continuous fiber systems, the fundamental mode of damage usually involves matrix cracking as the first sign of failure. The common hypothesis is that there exist in the basic material system inherent flaws of microscopic dimension, for instance, matrix voids, fiber-matrix debonds, etc. These microflaws, however, act as local stress risers when external loading is applied or a temperature change is incurred. At a certain location where the stress condition reaches a critical value, some dominant flaws begin to coalesce and form a large plane-crack. The size of such a crack is orders of magnitude larger than that of the microflaws. It is usually detectable at the macroscopic scale, e.g. by x-radiography, sonic scan and even visual inspection [1].

Because the matrix material and the matrix-fiber interface are weaker compared to the strength of the fibers, a macro-crack is almost always propagated through the matrix phase of the material. Hence, it is commonly labeled as a matrix crack.

Since laminates have a layered structure, an internal matrix crack cannot always undergo monotonic propagation; the crack may either be arrested or

0021-9983/84/03 0239--16 $4.50/0